

Gravity Waves generated by Sounds from Big Bang Phase Transitions

Tigran Kalaydzhyan and Edward Shuryak

*Department of Physics and Astronomy, Stony Brook University,
Stony Brook, New York 11794-3800, USA*

(Dated: December 7, 2024)

Inhomogeneities associated with the cosmological QCD and electroweak phase transitions produce hydrodynamical perturbations, longitudinal sounds and rotations. It has been demonstrated numerically by Hindmarsh *et al.* [1] that the sounds produce gravity waves (GW), and that this process does continue well after the phase transition is over. We further introduce a long period of the so-called *inverse acoustic cascade*, between the UV momentum scale at which the sound is originally produced and the IR scale at which GW is generated. It can be described by the Boltzmann equation, possessing stationary power and self-similar time-dependent solutions. If the sound dispersion law allows one-to-two sound decays, the exponent of the power solution is large and a strong amplification of the sound amplitude (limited only by the total energy) takes place. Alternative scenario dominated by sound scattering leads to smaller indices and much smaller IR sound amplitude. We also point out that two on shell phonons can produce a gravity wave and evaluate its rate using the so-called *sound loop diagram*.

I. INTRODUCTION

Thirty years ago, in a very influential paper Witten [2] discussed bubble dynamics, assuming that cosmic QCD phase transition is of the first order. Among other things, he pointed out that bubble coalescence/collisions produce inhomogeneities of the energy density, which lead to the gravity waves (GW) production. These ideas were soon further developed by Hogan [3] who identified relevant frequencies and provided the first estimates of the radiation intensity.

Hogan also was the first to mention the subject of this work – generation of the GW from the sound. Unfortunately, this idea was dormant for a very long time, being recently revived by Hindmarsh *et al.* [1], who found the hydrodynamic sound waves to be the dominant source of the GW. This paper had triggered our interest to the subject. Hindmarsh *et al.*, however, were performing numerical simulations of (variant of) the electroweak (EW) phase transition, in the traditional first order transition setting. We will discuss connection to this work in more detail in Section IV D.

Our paper refers to both QCD and EW transitions, with emphasis on the former case, both because of favorable observational prospects and our background. The main point of our paper is that, given a huge dynamical range of the problem, it is clearly impossible to cover it in a single numerical setting. We suggest to split the problem into distinct stages, each with its own physics, scales and technique. We will list them starting from the UV end of the spectrum, with momenta of the order of ambient temperature $k \sim T_c$ and ending at the IR end of the spectrum, $k \sim 1/t_{life}$, limited by the cosmological horizon (inverse to the Universe lifetime) at the radiation-dominated era:

- (i) production of sounds from inhomogeneities,
- (ii) inverse acoustic cascade, shifting the sound waves population toward the IR,

- (iii) the final conversion of sounds into GW

The stage (i) remains highly nontrivial, associated with the dynamical details of the QCD and EW phase transition. We will not be able to provide definite predictions on it at this point, and only make some comments on current status of the problem in Section VI.

The stage (ii) will be our main focus. It is in fact amenable to perturbative studies of the acoustic inverse cascade, consisting of sound decay/scattering events. Those are governed by the Boltzmann equation which has been already studied in literature on acoustic turbulence to certain extent. The stationary attractor solutions – known as Kolmogorov-Zakharov spectra – can be identified, as well as some time-dependent self-similar solution describing a spectrum profile moving across the dynamical range. Application of this theory allows to see how small-amplitude sounds at the UV end of the dynamical range are amplified and move toward smaller k .

The final step (iii) can be treated directly via a standard on-shell process for the *sound + sound* \rightarrow *GW* transition, to be calculated in Section V via a sound loop diagram.

Let us note that the studies of the QCD phase transition region, from the confined (or hadronic) phase to the deconfined Quark-Gluon Plasma (QGP) now constitute the mainstream of the heavy-ion physics. Experiments, done mostly at the RHIC in Brookhaven and now at CERN LHC, revealed that the matter above and near the phase transition seems to be a nearly perfect liquid with a small viscosity. Hydrodynamic description of the subsequent explosion – sometimes called the Little Bang – turns out to be very accurate.

Furthermore, initial state fluctuations create hydrodynamical perturbations of the Little Bang – the sounds. The long-wave ones can survive till the freezeout time without significant damping and are observed experimentally, in the correlation functions of the secondaries. These observations are in excellent agreement with the hydrodynamics see, e.g., [6, 7], and this ensures exis-

tence of the sound in the near- T_c matter. (Shorter-wave sounds, which do not survive till freezeout, were not yet observed, although there are suggestions [13] to use “magnito-sono-luminescence” processes $phonon + photon \rightarrow photon$ (or $dilepton$) to do so.)

There is, however, an important difference between the hydrodynamics in the heavy ion collisions (the “Little Bang”) and the early universe. The Reynolds number for QGP at RHIC is estimated [8] to be $Re_{RHIC} \sim 48\pi$ with the typical length scale $R_{Au} \sim 6$ fm, radius of the gold nucleus. Such a small Reynolds number would not allow instabilities – creating the turbulence – to be developed. In contrast, for the early universe, at, e.g., QCD phase transition,

$$Re_{EU} = \frac{t_{QCD} \cdot c}{R_{Au}} Re_{RHIC} \sim 10^{19}, \quad (1)$$

where we take the cosmological horizon to be a typical length scale (i.e. the Big Bang fireball is of order of 10 km size). In this case the turbulence can be fully developed, while the viscous forces are mostly irrelevant.

Thinking of other settings in nature, with a very large Reynolds number and strong turbulence, one may take an example of the Sun, or stars in general. In this case the acoustic waves are generated by the convection. The energy spectrum of the acoustic waves was obtained from various models [9], and its most prominent feature is the power spectrum with inverse power of momentum, except a flat peak at its smallest values k_{IR} .

The analogy between the early Universe and the Sun cannot be used in a straightforward way, for several reasons. First of all, Sun is near-stationary, with well defined source and sink. Second, the Sun’s plasma is strongly influenced by long-range magnetic fields, forming flux tubes described by magneto-hydrodynamics (MHD). The QGP near T_c can be described as a plasma with both electric and magnetic objects [11, 12]. However, the screening length of both electric and magnetic fields is generally close to the microscopic scale $1/T$. Dynamics of the electric flux tubes do exist, near and below T_c , and it can lead to “string balls” [10]. While those excitations can lead to interesting phenomena, perhaps to sound generation, they clearly cannot be long range, i.e. important at distance scales much larger than the micro scale $1/T$.

Finally, let us also mention papers by Kovtun *et al.* [14, 15] and subsequent works, which help us to think about the sound interactions. A particular effect they calculated is the correction to the viscosity due to sounds, i.e the “loop viscosity”, appearing technically as a sound loop in the energy-momentum correlator $G^{xyxy}(k_\alpha)$. This effect lead us to think about the sound decay and/or GW formation (although their kinematics is different from what we have considered).

II. FREQUENCIES, OBSERVATIONAL METHODS AND EXPERIMENTAL LIMITS ON THE COSMIC GRAVITY WAVES

Let us briefly mention the numbers related to the QCD and EW transitions. Step one is to evaluate redshifts of the transitions, which can be done by comparing the transition temperatures $T_{QCD} = 170$ MeV and $T_{EW} \sim 100$ GeV with the temperature of the cosmic microwave background $T_{CMB} = 2.73$ K. This leads to

$$z_{QCD} = 7.6 \times 10^{11}, \quad z_{EW} \sim 4 \times 10^{14}. \quad (2)$$

At the radiation-dominated era, to which both QCD and EW era belong, the solution to Friedmann equations leads to a well known relation between the time and the temperature [24]

$$t = \left(\frac{90}{32\pi^3 N_{DOF}(t)} \right)^{1/2} \frac{M_P}{T^2}, \quad (3)$$

where M_P is the Planck mass and $N_{DOF}(t)$ is the effective number of bosonic degrees of freedom (see details in, e.g., PDG Big Bang cosmology).

Plugging in the corresponding T one finds the the time of the QCD phase transition to be $t_{QCD} = 4 \times 10^{-5}$ s, and electroweak $t_{EW} \sim 10^{-11}$ s. Multiplying those times by the respective redshift factors, one finds that the t_{QCD} scale today corresponds to about 3×10^7 s = 1 year, and the electroweak to 5×10^4 s = 15 hours.

The cosmological horizon provides a natural infrared cutoff on the gravitational radiation wavelength. At the radiation-dominated era it is inversely proportional to the time, so the estimates above give a cutoff on the periods of the gravitational waves in the present time. GW from the electroweak era are expected to be searched for by future space GW observatories such as eLISA: discussion of their potential sensitivity can be found elsewhere. The observational tools for GW at the period scale of *years* are based on the long-term monitoring of the millisecond pulsar phases, with subsequent correlation between all of them. The basic idea is that when GW is falling on Earth and, say, stretches distances in a certain direction, then in the orthogonal direction one expects distances to be contracted. The binary correlation function for the pulsar time delay is an expected function of the angle θ between them on the sky. There are existing collaborations – North American Nanohertz Observatory for Gravitational Radiation, European Pulsar Timing Array (EPTA), and Parkes Pulsar Timing Array – which actively pursue both the search for new millisecond pulsars and collecting the timing data for some known pulsars. It is believed that about 200 known millisecond pulsars constitute only about 1 percent of the total number of them in our Galaxy. We also note that the current bound on the GW energy density for the frequencies in interest, $f \approx \text{year}^{-1}$, is [16]

$$\Omega_{GW}(f = 2.8\text{nHz}) \cdot (h_0/0.73)^2 < 1.3 \times 10^{-9}, \quad (4)$$

where Ω_{GW} is, as usually, the total energy density of GW relative to the critical energy density and

$$\Omega_{\text{GW}}(f) = d\Omega_{\text{GW}}/d(\ln f). \quad (5)$$

This bound should constrain possible models of the GW production in the early Universe. (Note that at the time of QCD (EW) transition Ω_{rad} is about 4 (15) orders of magnitude larger due to its dependence on the scaling factor $a(t)$, so the aforementioned limit is weaker for those times)

Rapid progress in the field, including better pulsar timing and formation of a global collaborations of observers, is expected to improve the sensitivity of the method, perhaps making it possible in a few year time scale to detect GW radiation, either from the QCD Big Bang GW radiation we discuss, or that from colliding supermassive black holes.

III. PRELIMINARY DISCUSSION OF SOUND-TO-GW TRANSITION

For comparison, let us start with the Little Bang – heavy-ion collision. As one of us suggested many years ago [17], production of penetrating probes – photons and dileptons – not only provide a look inside the quark-gluon plasma, but is even somewhat enhanced. The rate of, e.g., photon production due to the strong Compton scattering and annihilation $qg \rightarrow q\gamma, \bar{q}g \rightarrow \bar{q}\gamma, \bar{q}q \rightarrow g\gamma$ is

$$dN_\gamma/d^4x \sim \alpha\alpha_s T^4 \quad (6)$$

and thus the photon accumulated density normalized to the entropy density of matter $s_{\text{QGP}} \sim T^3$ is of the order of

$$\frac{\int dt dN_\gamma/d^4x}{s_{\text{QGP}}} \sim \alpha\alpha_s(t_{\text{life}} T), \quad (7)$$

where t_{life} is the fireball lifetime. Small QED and QCD coupling constants in front are thus partly compensated by large $(t_{\text{life}} T) \gg 1$, called “macro-to-micro ratio”, which will repeatedly appear below. This factor represents a long accumulation time of the photon production, and it is about one order of magnitude in heavy ion collisions.

Similar logic holds for the gravitational radiation from matter constituents. The characteristic micro scale of the plasma is its temperature T . At the thermal (the high-frequency) end of the spectrum, $\omega \sim T$, one finds the fraction of GW radiation to the total energy density $T^{00} \sim N_{\text{DOF}} T^4$ to be given by a similar expression,

$$\Omega_{\text{GW}} \sim \left(\frac{T}{M_P}\right)^2 (t_{\text{life}} T), \quad (8)$$

where the first factor is the corresponding effective gravitational coupling, which is very small since $T/M_P \sim 10^{-20} - 10^{-17}$ in our case. The macro-to-micro factor

is a large enhancement factor, which can be readily obtained from (3) and in fact contains an inverse of the ratio just mentioned, so

$$tT \sim \frac{M_P}{T} \cdot \frac{1}{N_{\text{DOF}}^{1/2}} \sim 10^{16} - 10^{19}. \quad (9)$$

This fraction cannot, however, cancel all powers of M_P the the coupling factors, so the gravitational radiation directly from plasma particles is strongly suppressed.

While matter is mostly made of various partons with $k \sim T$, it also contains long wavelength collective modes, the hydrodynamical sounds. Thermal occupations of plasma partons are $n_k = O(1)$, but for sounds, even in equilibrium, their occupation factors for small frequencies are much larger, $n_k \sim T/k \gg 1$. Out-of-equilibrium phenomena we will study below lead to even much higher amplitudes of hydrodynamical perturbations. (Anyone who flied by plane through a region of turbulence is well aware of this fact.)

The amplitudes grow toward smaller k in an inverse acoustic cascade. The sound momenta/frequencies are however limited from below, and thus the sound intensities n_k are limited as well. The most obvious infrared cutoff is by the inverse lifetime of the Universe, $\omega > 1/t_{\text{life}}$: more precise cutoff is due to a collision rate which we will discuss below.

The sound conversion to GW happens via two-to-one transition, and therefore its rate is enhanced *quadratically* $\sim n_k^2$. The peak in the sound intensity squared will be repeated in the GW spectrum. The more it moves to the IR the stronger will be the GW signal, and better chances we have to eventually observe it.

Summarizing this section: only strongly enhanced out-of-equilibrium sounds may potentially produce observable level of GW. The problem is reduced to an estimate of the sound level or κ_{sound} . To illustrate that this task is highly non-trivial we note that the loudest sounds on Earth have nothing to do with the equilibrium atmosphere but with the thunderstorms, earthquakes or sea waves falling ashore.

IV. ACOUSTIC TURBULENCE

The idea of turbulence, either driven or free, started from hydrodynamics of fluids. Kolmogorov proposed the famous stationary power solutions. For the weak turbulence, governed by the Boltzmann equation, such solutions were developed by Vladimir Zakharov and collaborators to many different problems, see e.g. a review in a book Ref. [18]. Also a turbulent cascade in cosmology was suggested to appear after the pre-heating stage of inflation [19]: that was for a scalar field with quartic interaction, and the cascade considered there was *direct*, propagating into UV, towards the large momenta k . Consideration of *inverse* cascade to IR, more similar to our case, was done for gluons, in classical gauge theories,

see e.g. [20], with and without expansion. The inverse acoustic cascade terminating in GW formation, to our knowledge, has been not discussed before.

A. Scenario 1: sound decays

The key parameter of the theory to be presented is the $O(k^3)$ corrections to the sound dispersion law, since the sound cascade depends on them in a crucial way. Although they are not known experimentally for the sound near the QCD phase transition, it has been derived for a strongly coupled plasma of the $\mathcal{N}=4$ super-Yang-Mills theory, through the AdS/CFT correspondence. It is widely believed that those should be similar, at least qualitatively. Not going into details, the known terms in the sound dispersion curve, up to $O(k^6)$ accuracy, are [4]

$$\frac{\omega}{2\pi T} = \pm \frac{\tilde{k}}{\sqrt{3}} \left[1 + \left(\frac{1}{2} - \frac{\ln 2}{3} \right) \tilde{k}^2 - 0.088 \tilde{k}^4 \right] - \frac{i\tilde{k}^2}{3} \left[1 - \frac{4 - 8 \ln 2 + \ln^2 2}{12} \tilde{k}^2 - 0.15 \tilde{k}^4 \right], \quad (10)$$

where $\tilde{k} \equiv k/(2\pi T)$. The crucial observation is that the $O(k^2)$ correction in the first bracket of (10) has a *positive* coefficient, let us call it a^2 , such that

$$\omega(k) = \pm c_s k (1 + a^2 k^2) + \dots \quad (11)$$

This allows for $1 \leftrightarrow 2$ transitions between the sound waves, in particular, a decay of a harder phonon into two softer ones. Although this is in principle known, for completeness let us remind the kinematics of this process.

The momentum conservation $\vec{k} = \vec{k}_1 + \vec{k}_2$ allows to introduce a parameter $x \in [0, 1]$ and a vector \vec{q}_\perp such that \vec{k}_1, \vec{k}_2 will have longitudinal components along \vec{k} denoted by $\vec{k}_1^\parallel = \vec{k} \cdot x$, $\vec{k}_2^\parallel = \vec{k} \cdot (1 - x)$ and the transverse ones $\vec{k}_{1,2}^\perp = \pm \vec{q}_\perp$, where plus (minus) are for \vec{k}_1 (\vec{k}_2). The energy conservation,

$$\omega(k) = \omega(k_1) + \omega(k_2), \quad (12)$$

can be simplified using the fact that the dispersive correction is small in the range we are interested in,

$$(ak) \ll 1. \quad (13)$$

Realizing that the transverse momentum is proportional to it and thus it is also small, one may simplify energy conservation further. The resulting value of the transverse momentum, for a given value of longitudinal momentum fraction x , is

$$\frac{q_\perp}{k} = (ak)\sqrt{6x(1-x)}. \quad (14)$$

B. Scenario 1: Boltzmann equation and its stationary solution

One can further argue that, due to the Goldstone nature of sounds, their interaction matrix element at small momenta (IR) must be proportional to the product of all momenta,

$$|V(k, k_1, k_2)|_{\text{IR}}^2 = bk \cdot k_1 \cdot k_2, \quad (15)$$

where b is a constant. Having in mind this matrix element, the phase space of the decay, one can write down a kinetic equation including all $1 \leftrightarrow 2$ transitions. The details can be found e.g. in a book Ref. [18]. Let us present here only the final form of the Boltzmann equation with the assumption of the isotropy of spectra and the angle integrations performed,

$$\frac{1}{4\pi b} \frac{\partial n_k}{\partial t} = \int_0^k dk_1 k_1^2 (k - k_1)^2 [n_{k_1} n_{k-k_1} - n_k (n_{k_1} + n_{k-k_1})] - 2 \int_k^\infty dk_1 k_1^2 (k - k_1)^2 [n_k n_{k_1-k} - n_{k_1} (n_k + n_{k_1-k})]. \quad (16)$$

In spite of relatively complicated form of the equation, it has simple stationary power solutions, generally known as Zakharov's spectra [18],

$$n_k \sim k^{-s}, \quad s_{\text{decay}} = 9/2 \quad (17)$$

This power solution is stable ‘‘attractor’’ solution. Numerical simulations, starting from a variety of out-of-equilibrium distributions, have been shown to approach this spectrum rather rapidly, again see Ref. [18] for details.

One comment is that the case of three-dimensional space $d = 3$ is exceptional: dimensional dispersion curve parameter a does appear in the collision term, but drops out after the angular integration and do not appear in r.h.s. of (16). Therefore, the resulting index in this case is the same as given by the Kolmogorov theory by his dimensional argument, although it is not so for a general $d \neq 3$.

The sound spectrum with such a large index s should work as a powerful amplifier of the sound amplitude in the IR. This strong amplification of the sound by the acoustic cascade is the central point of the present work.

The total energy density contained in the sounds with all k is

$$\epsilon_{\text{sound}} = \int \omega_k n_k 4\pi k^2 dk. \quad (18)$$

After putting into it the solutions for scenario 1 (with decays) and index $s = 9/2$ one finds that the normalization is concentrated at the IR end of the spectrum, more specifically, as $k_{\text{IR}}^{-1/2}$. We introduce a normalization parameter P_{sound} ,

$$\epsilon_{\text{sound}} = P_{\text{sound}} T^4 \quad (19)$$

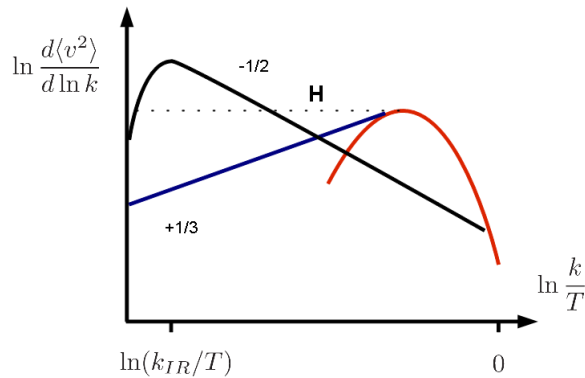


FIG. 1: Schematic power spectrum of the sound waves versus their momentum, or $\log(k/T)$. The r.h.s. is the UV end of the dynamical range, (red) curve on the right corresponds to the spectrum produced soon after the phase transition period. The spectrum later evolves toward the attractor solutions, shown by the black and blue lines. Scenario 1 has the effective power $-1/2$ starting from a certain scale, and the scenario 2 has power $+1/3$, as shown near the lines. The horizontal dashed line, marked by H, is the “Hindmarsh scenario”, see the text.

which is roughly a fraction of energy contained in the sounds relative to the power of the UV scale in plasma (Numerical coefficients in the energy density can be included later, if needed: we omit them in order to keep the expressions simple.)

In the first scenario, with decays, the index is (17) and the normalization is dominated by the IR end. The normalized solution thus looks as follows

$$n_k = \frac{P_{sound}}{8\pi c_s} \left(\frac{k_{IR}}{T}\right)^{1/2} \left(\frac{T}{k}\right)^{9/2}. \quad (20)$$

C. Scenario 1: The collision rate

So far we assumed that the total time t available – limited by cosmological horizon in the QCD or EW phase transition eras – is sufficiently long for the attractor solution to be fully developed, all the way through the whole dynamical range. While we do not attempt in this work to do out-of-equilibrium simulation of the cascade, we nevertheless make some preliminary estimates on the scales spanned by the cascade and obtain certain restrictions on the GW production rate.

Let us define the collision time via *one* of the terms in the Boltzmann equation (16), for example

$$\frac{1}{\tau_k} = \frac{\dot{n}_k}{n_k} = \frac{4\pi b}{n_k} \int_{k_{IR}}^k dk_1 k_1^2 (k - k_1)^2 n_{k_1} n_{k-k_1}, \quad (21)$$

where the dot denotes a time derivative.

Let us now substitute into the r.h.s. the assumed normalized attractor solution (20) and integrate up to some scale k . (Of course, one needs to consider only one of the terms, because the complete collision term vanishes on the solution.) One finds the combination of the scattering time and momentum

$$\tau_k k = \frac{8c_s}{P_{sound} b T^4} \left(\frac{k}{k_{IR}}\right)^{1/2}. \quad (22)$$

The scattering parameter is formed in UV so perhaps $bT^4 \sim 1$ and the magnitude of the r.h.s. is defined mostly by $1/P_{sound}$ which one can optimistically assume to be 10^2 or so.

In particular, at the very IR end, the scattering happens at times of about hundred periods or so: and since at the IR end of the spectrum the horizon time we assumed to be $t_{life} \cdot k_{IR} \sim 1$ one finds that the acoustic cascade cannot reach the IR end. However, according to this estimate, it may reach say k of few hundreds of k_{IR} .

D. Scenario 1: Self-similar solution

To describe the time evolution of the initial sound distribution function, we use the idea of self-similarity known in similar applications like [19]. The self-similar solution of the Boltzmann equation has a generic form

$$n_k = (Tt)^\alpha f_s \left[(Tt)^\beta \cdot \frac{k}{T} \right] \quad (23)$$

defined by two exponents α, β and the profile function $f_s[x]$, which is assumed to retain its shape during the evolution. One can think of it as a “soliton” moving in the space of logarithmic scales, $\log(k/T)$, $\log(Tt)$, in momentum and time, from UV to IR, such that

$$\beta \log(Tt) + \log\left(\frac{k}{T}\right) = \text{const} = \log x. \quad (24)$$

The qualitative expected shape of the function $f_s[x]$ should have a maximum at $x_{max} \sim \tau_k k$ given in (22), a power slope with an exponent given by the attractor solution at larger $x > x_{max}$, and a rapid decay at smaller $x < x_{max}$. Approximating the latter by a sharp cutoff $f_s[x] \sim \theta(x - x_{max})/x^s$ and substituting this form into the energy normalization (18), one finds the first relation between indices,

$$\alpha - 4\beta = 0. \quad (25)$$

The second one comes from the Boltzmann equation (16),

$$\alpha - 1 = 2\alpha - 5\beta, \quad (26)$$

so the exponents turn out to be unambiguously fixed,

$$\alpha = 4, \quad \beta = 1. \quad (27)$$

Let us now compare those general predictions with the results of the numerical simulations done in Ref. [1]. In all those – and many other – works it is assumed that the cosmic phase transitions have so-to-say maximal strength: that they are of the first order and that the latent heat is comparable to the energy density. The order of the EW phase transition depends on the Higgs mass and, since we now know the Higgs mass value, the EW phase transition should be only a crossover within the standard model. There exist certain extensions of the standard model, not excluded by current LHC experiments, which will provide the first order transition: this option is the motivation for Ref. [1] and related works.

In Ref. [1], the transition was simulated via hydrodynamics coupled to the Higgs field, and the specific finding of that work is the GW generation process which continues – with about constant rate – long after the phase transition is over. Their further studies had shown that GW originates from the long-wavelength sound waves, not from the rotational modes. Of course, in a single simulation it is only possible to cover a small part of the vast dynamical range (which will be about 18 decades for QCD): this work covers two decades, from $k \sim T$ to $k \sim 10^{-2}T$. This is simply because a large difference between the natural IR (size of the box) and UV (lattice spacing) cutoff would require a large number of discretization points. Another very strong limitation is related to the time of the evolution followed. As we already noted, the acoustic cascade is a very slow process, and it can only be studied by a long-time calculation.

The most important quantity calculated from their hydrodynamical output is the spectrum of the fluid velocity squared, $dV^2/d \log k$ (see Fig. 4 in [1]). The spectra allowed them to conclude – and this triggered in fact our studies – that the sounds dominated energetically the rotational modes.

Since the energy of the sound waves, to the second order, is the unperturbed density of matter times the fluid velocity squared $(\epsilon + p)_0 V^2$, one can relate it to the sound wave occupation numbers as follows

$$\frac{dV^2}{d \log k} \frac{dk}{k} \sim \omega_k n_k k^3 \frac{dk}{k}. \quad (28)$$

Results of these simulations provide, in principle, the initial sound power spectrum, from which the inverse acoustic cascade starts evolving. (It is schematically shown by the red curve on the right in Fig. 1.) An important parameter one obtains from these simulations is the total fraction of the sound energy P_{sound} , the integrated power spectrum, which in their case is as large as

$$P_{sound} \sim 10^{-2}. \quad (29)$$

A more precise value depends on the behavior of the spectrum at smaller k , not yet available. The calculated spectrum is approximately flat (k -independent), and Hindmarsh *et al.* assumed it to be the case all the way to IR. (in our sketch in Fig. 1 this scenario is shown by the dashed horizontal curve marked by H.)

More accurately, one observes that the spectrum of Hindmarsh *et al.* has a shallow maximum at their characteristic dynamical scale – the distance between bubbles. Should this calculation be extended to smaller k , we think it is inevitable that the spectrum will be cut off in IR exponentially. There is simply not enough time for the sound cascade to evolve.

E. Scenario 2: rescattering

In a situation, when the dispersive correction coefficient we denoted a^2 in (11) is negative, binary decays of sound are forbidden. In this case one should consider the second order perturbation theory, involving higher order scattering processes $2 \leftrightarrow 2$ and the analysis is much more involved.

According to Ref. [18] such Boltzmann equations also have power solutions, with a different indices

$$s_{nondecay} = 10/3, 11/3 \quad (30)$$

The exact values of those are not important: the key is that they are in the strip

$$3 < s < 4 \quad (31)$$

As a result, the energy integral (18) is *not* defined at the IR end, but at the UV. However, in the case of rescattering there appears another integral of motion – the particle number

$$N = \int n_k 4\pi k^2 dk \quad (32)$$

which *is* dominated by the IR end. Such cascades, driven by particle number normalizations, are usually called “the particle number cascade”. Self-similar solution will have normalization relation between exponents,

$$\alpha - 3\beta = 0. \quad (33)$$

The second constraint on α and β from the Boltzmann equation requires a more subtle analysis and will be considered elsewhere. The power spectrum dependence on the scale k for these two scenarios at a fixed time moment is schematically shown in Fig. 1.

V. GENERATION OF GRAVITY WAVES

A. The spectral density of the stress tensor correlator

General expressions for the GW production rate are well known, and we will not reproduce them here, proceeding directly to the main object one has to calculate, the two-point *correlator of the stress tensors*

$$G^{\mu\nu\mu'\nu'} = \int d^4x d^4y e^{ik_\alpha(x^\alpha - y^\alpha)} \langle T^{\mu\nu}(x) T^{\mu'\nu'}(y) \rangle. \quad (34)$$

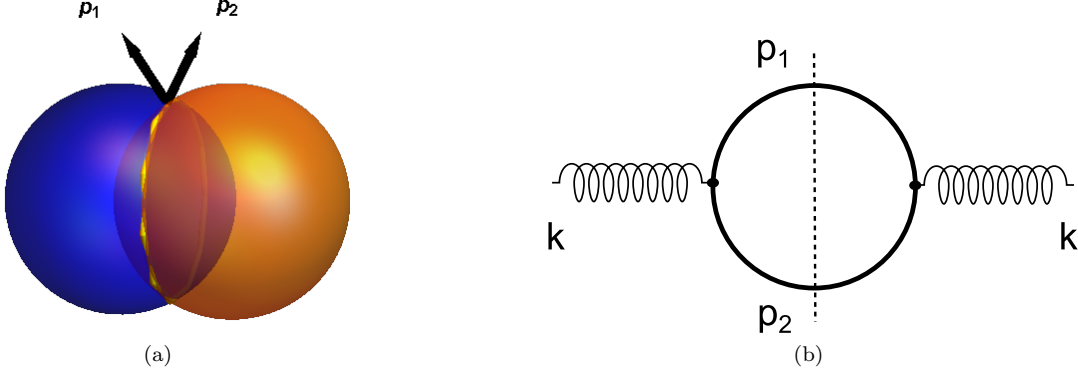


FIG. 2: (a) Sketch of the collision of two sound waves (b) The diagram and the cut described in the text. External legs are gravity waves (gravitons), and the sounds (phonons) are in the loop.

Note that while the Big Bang is homogeneous in space, so 3-momentum can well be defined and conserved, but it is time-dependent. We will however still treat it as quasi-static, with well defined frequencies of perturbations, with a cutoff at the lowest end $\omega < 1/t_{life}$.

Using hydrodynamical expression for the stress tensor,

$$T^{\mu\nu} = (\epsilon + p) u^\mu u^\nu + g^{\mu\nu} p, \quad (35)$$

and expanding it in powers of a small parameter – the sound amplitude – one can identify terms related to the sound wave. Associating the zeroth order terms with the matter rest frame, one introduces the first order velocities by

$$u^\mu = (1, 0, 0, 0) + \delta u_{(1)}^\mu \quad (36)$$

and one expands the stress tensor to the second order as

$$\delta T_{(2)}^{\mu\nu} = (\epsilon + p)_{(0)} \delta u_{(1)}^\mu \delta u_{(1)}^\nu + (\epsilon + p)_{(2)} \delta^{\mu 0} \delta^{\nu 0} + p_{(2)} g^{\mu\nu}. \quad (37)$$

The correlator is to be coupled to the metric perturbations $h_{\mu\nu} h_{\mu'\nu'}$ and we are interested in indices corresponding to two polarizations of GW transverse to its momentum k_α . Such components are only provided by the term with velocities, and thus we focus on

$$\int d^4x d^4y e^{ik_\alpha(x^\alpha - y^\alpha)} \langle \delta u^\mu(x) \delta u^\nu(x) \delta u^{\mu'}(y) \delta u^{\nu'}(y) \rangle, \quad (38)$$

where we dropped the overall factor $(\epsilon + p)_{(0)}^2$ and subscripts “(1)” for the first order terms.

The next step is to split four velocities into two pairs, for which we use the “sound propagators”,

$$\Delta^{mn}(p^0, \vec{p}) = \int d^4x e^{ip_\mu x^\mu} \langle \delta u^m(x) \delta u^n(0) \rangle, \quad (39)$$

where we changed indices to the Latin ones emphasizing that those are only spatial. In these terms the correlator

in question is a loop diagram shown in Fig. 2(b). Similar loop diagrams were derived and discussed in connection to fluctuation-induced or loop corrections to hydrodynamical observables: for a recent review of the results, standard definitions and relations see [15].

Time dependent Green’s functions can be chosen differently depending on the assumed boundary conditions on the time dependence. The most natural Green’s functions for the sounds are the retarded one Δ_R , which has only poles in a half of the complex energy $E = p^0$ plane, corresponding to the sound dissipation, and the symmetric one Δ_S , which has all 4 possible poles. In equilibrium, they are related to each other by the so-called Kubo-Martin-Schwinger (KMS) relation ($E = p^0$),

$$-\Delta_S = (1 + 2n_B(E)) \text{Im} \Delta_R \underset{E \ll T}{\approx} \frac{2T}{E} \text{Im} \Delta_R, \quad (40)$$

where $n_B(E)$ is the equilibrium Bose distribution. This expression shows that $\text{Im} \Delta_R$ corresponds to a single phonon quantum, and the Δ_S to a wave with proper occupation numbers. It also suggests generalization to an out-of-equilibrium case we will use, i.e. introduction of new rescaled function

$$-\tilde{\Delta}_S = 2n(E) \text{Im} \Delta_R, \quad (41)$$

containing out-of-equilibrium occupation number $n(E)$, which is assumed to be much larger than the quantum term 1 in (40), which is therefore dropped. The explicit expression to be used takes the form

$$\tilde{\Delta}_R^{mn} = \frac{1}{(\epsilon + p)_{(0)}} \frac{p^m p^n}{p^2} \frac{E^2}{(E^2 - p^2 c_s^2) + i\tilde{\gamma} p^2 E}, \quad (42)$$

where notations are 3-dimensional, e.g. $p^2 = \vec{p}^2$. The dissipation lifetime parameter is related to the shear viscosity,

$$\tilde{\gamma} = \frac{4}{3} \cdot \frac{\eta}{\epsilon + p}. \quad (43)$$

Now one can perform the Fourier transformation and represent the correlator as a standard field theory loop diagram. The imaginary part of the correlator, as usually, corresponds to the unitarity cut of the loop into two parts, or *probability* of the corresponding sounds merging process,

$$\frac{\text{Im } G^{mm'nn'}(k)}{(\epsilon + p)_{(0)}^2} = \int \frac{d^4 p}{(2\pi)^4} n(p^0) \text{Im } \tilde{\Delta}_R^{mm'}(p) n(k^0 - p^0) \text{Im } \tilde{\Delta}_R^{nn'}(k - p) \quad (44)$$

Multiplied by the Newton coupling constant and taken on-shell $k_\alpha^2 = 0$ this will give us the rate of the *sound+sound* \rightarrow GW process. Note, that the unitarity cut puts also on shell both sound lines.

B. Sounds to GW: kinematics

One sound wave obviously cannot produce a GW: (i) the dispersion relation for the sound is $\omega = c_s k$, different from that of the GW, $\omega = k$; (ii) polarization of the sound wave is a longitudinal vector, while it should be a transverse tensor for GW.

Two on-shell sound waves can do it. Using notations $p_1^\mu + p_2^\mu = k^\mu$ one writes GW on-shell condition $(k^\mu)^2 = 0$ as

$$c_s^2(p_1 + p_2)^2 = p_1^2 + p_2^2 + 2p_1 p_2 \cos(\theta_{12}), \quad (45)$$

where c_s, θ_{12} are the sound velocity and an angle between the two sound waves, respectively. In terms of such an angle there are two extreme configurations. The first is a “symmetric case”, $p_1 = p_2$, corresponding to a minimal angle. For $c_s^2 = 1/3$ this angle is $\theta_{12} = 109^\circ$. The second, “asymmetric case”, corresponds to anticollinear vectors \vec{p}_1, \vec{p}_2 , $\theta_{12} = 180^\circ$. Important difference from the usual textbook relativistic-invariant cases is that various θ_{12} are allowed by kinematics in our case, not only $\theta_{12} = 0^\circ$, which is due to the fact that $c_s < 1$.

Since the sources of sounds are of microscopic size $\sim 1/T$ much smaller than time t of observations, sound waves from them have the form of spherical pulses expanding with the speed of sound. A sketch of the intersection of two such sound spheres is shown in Fig. 2: it is clear that the angle between the sound momenta runs with time over the region allowed for the GW formation.

However, at least at the momentum range in which sounds are weak and the lowest order process $2 \rightarrow 1$ dominates the GW production, one may not think about specific hydrodynamical configurations, but simply view it as incoherent set of plane waves with certain occupation number n_k .

C. GW generation rate

We proceed to calculation of the “unitarity cut” of the stress tensor correlator, in which both sound propagators are taken on-shell,

$$E_p = \pm c_s p - \frac{i}{2} \tilde{\gamma} p^2. \quad (46)$$

One can check that the viscous damping is small, $\tilde{\gamma} k \ll 1$, so it is only needed to go around a pole on the real axis in a correct way. The matrix element is given by a sum over the GW polarizations,

$$\langle \text{Im } G \rangle = \sum_{i=+, \times} \epsilon_i^{*mn} \text{Im } G_{mm'nn'} \epsilon_i^{m'n'}, \quad (47)$$

where the polarization matrices can be chosen to be

$$\epsilon_+^{mn} = \frac{1}{\sqrt{2}} \begin{pmatrix} 0 & 0 & 0 & 0 \\ 0 & 1 & 0 & 0 \\ 0 & 0 & -1 & 0 \\ 0 & 0 & 0 & 0 \end{pmatrix}, \quad \epsilon_\times^{mn} = \frac{1}{\sqrt{2}} \begin{pmatrix} 0 & 0 & 0 & 0 \\ 0 & 0 & 1 & 0 \\ 0 & 1 & 0 & 0 \\ 0 & 0 & 0 & 0 \end{pmatrix}$$

in the transverse traceless gauge, for a plane wave propagating along the third coordinate. Alternatively, one can use a more general standard replacement for the sum,

$$\begin{aligned} \sum_{\text{polar.}} \epsilon_{mn}^* \epsilon_{m'n'} &= \frac{1}{2} [(\delta_{mm'} \delta_{nn'} + \delta_{mn'} \delta_{nm'} - \delta_{mn} \delta_{m'n'}) \\ &- (\delta_{mm'} \hat{k}_n \hat{k}_{n'} + \delta_{mn'} \hat{k}_m \hat{k}_{m'} - \delta_{mn} \hat{k}_{m'} \hat{k}_{n'}) \\ &- (\delta_{nn'} \hat{k}_m \hat{k}_{m'} + \delta_{nm'} \hat{k}_n \hat{k}_{n'} - \delta_{nm} \hat{k}_{m'} \hat{k}_n) \\ &+ \hat{k}_m \hat{k}_n \hat{k}_{m'} \hat{k}_{n'}]. \quad (48) \end{aligned}$$

Next, the loop momentum integral is customary rewritten as $\int d^4 p_1 d^4 p_2 \delta^4(p_1 + p_2 - k) \dots$, and the integral over the energies is taken first using the poles of the denominator. The pole residua are the numerator on shell (46) divided by the usual $2E_p = 2c_s p$ as for a relativistic particle. Eliminating integral over \vec{p}_2 and 3 delta functions one is left with a single delta function expressing conservation of energy in the process,

$$\delta \left[k - c_s p_1 - c_s \sqrt{p_1^2 + k^2 - 2p_1 k \cos \alpha_{1k}} \right], \quad (49)$$

where α_{1k} is an angle between the total (GW) momentum \vec{k} and \vec{p}_1 . So far the steps are similar to a standard calculation of the phase space for particle decays, in which one can go to c.m. frame, impose a constraint on momenta from the energy conservation and reduce the problem to simple angular integrals. Unfortunately, in the problem at hand we deal with a massless graviton and we also lack relativistic invariance, which makes this procedure useless. Therefore, all three integrals, $d^3 p_1 = p_1^2 dp_1 d \cos \alpha_{1k} d\phi$, should be done explicitly.

Let us first check the integration limits on p_1 . From the equations on the energy and momentum conservation one gets

$$\cos(\alpha_{1k}) = \frac{1}{2p_1} \left(k - \frac{k}{c_s^2} + 2 \frac{p_1}{c_s} \right), \quad (50)$$

and demanding it to be within the range $[-1, 1]$ one can constrain the momentum p_1 to be between the minimal and maximal values,

$$p_1^{max} = \frac{1 + c_s}{2c_s} k, \quad p_1^{min} = \frac{1 - c_s}{2c_s} k. \quad (51)$$

Zero of the argument of the delta function (49) falls into this range, so one can simply replace all p_1 by this zero.

After summing over two polarizations of the GW and taking into account occupation numbers $n(p)$ for the sounds, the integral can be written as

$$\begin{aligned} \langle \text{Im } G \rangle = & \int n(p_1) n(k/c_s - p_1) p_1^2 dp_1 d \cos \alpha_{1k} d\phi \cdot \frac{c_s + 1/c_s - 2 \cos \alpha_{1k}}{2(c_s \cos \alpha_{1k} - 1)^2} \cdot \delta \left[p_1 - \frac{k(c_s^2 - 1)}{2c_s \cos \alpha_{1k} - 1} \right] \\ & \times \frac{c_s^2 p_1^2}{2c_s p_1} \cdot \frac{c_s^2 (k/c_s - p_1)^2}{2(k - c_s p_1)} \cdot \frac{1}{2} (1 - \cos^2 \alpha_{1k}) \left[1 - \left(\frac{k - p_1 \cos \alpha_{1k}}{k/c_s - p_1} \right)^2 \right], \end{aligned} \quad (52)$$

where the first line contains the Jacobian for the delta-function, and the second line comes from the sound propagators (42) and the summation formula (48).

To make sense of the integral (52), which determines the GW generation rate, let us consider three simple cases. If the distribution is flat, $n(p) = A$, then the integral (52) is proportional to the volume of the phase space and equals to

$$\langle \text{Im } G \rangle_{p^0} = \frac{A^2 \pi k^4 (1 - c_s^2)^2}{120 c_s^2}. \quad (53)$$

In the case of thermal equilibrium, $n(p) = Ap^{-1}$, we get a lengthy expression, which can be simplified for $c_s = 1/\sqrt{3}$,

$$\langle \text{Im } G \rangle_{p^{-1}} = \frac{A^2 \pi k^2}{9} \left(\sqrt{3} - 3 \operatorname{arccoth} \sqrt{3} \right). \quad (54)$$

Finally, for the inverse cascade case (20), the integral is equal to

$$\langle \text{Im } G \rangle_{p^{-9/2}} = \frac{k_{\text{IR}} T^8 P_{\text{sound}}^2}{k^5} \cdot \frac{(7967 - 4608\sqrt{3})}{7680\sqrt{6}\pi}. \quad (55)$$

In the case of self-similar solution (23, 27) with a cutoff $k_{\text{IR}}(t) \propto 1/t$ and $s = 9/2$ one obtains

$$\langle \text{Im } G \rangle(t) \propto \frac{k_{\text{IR}}(t) T^8 P_{\text{sound}}^2}{k^{5t}}, \quad k \gg k_{\text{IR}} \quad (56)$$

and some small value at $k \lesssim k_{\text{IR}}$ which depends on the way the sound spectrum decreases towards longer wavelengths. Here we used the fact that the loop momentum p_1 is comparable to k from the limits (51) and hence the cutoff in the sound spectrum will be translated to the cutoff in the GW spectrum through the integral (52).

A detailed prediction of the GW yield requires a knowledge of the shape of the profile $f_s[x]$, which we now do

not have yet. Qualitatively, the maximum of the radiation power follows the maximum of f_s , which should be defined by the collision rate (22)

$$\frac{d\Omega_{\text{GW}}}{d \log(k)} \sim \left(\frac{T}{M_P} \right)^2 \left(\frac{T}{k} \right)^2 (f_s[kt])^2 \quad (57)$$

where the first factor represents the smallness of the coupling, the second one is the large space-time factor, and the last the occupancies. When k reaches the IR cutoff given by the Hubble scale, $k = k_{\text{IR}}$, the first two factors nearly cancel each other: the largest parameter, Planck mass, is gone. However, as we explained above, one has to stop at some finite distance from the Hubble scale in the momentum space, because of a not sufficient collision rate. The magnitude of f_s at its maximum is basically given by the parameter P_{sound} , the fraction of the matter energy stored in sounds: thus the GW yield is proportional to P_{sound}^2 . With optimistic value of $P_{\text{sound}} \sim 10^{-2}$ one may perhaps reach $\Omega_{\text{GW}} \sim 10^{-6}$ which is not too far from current upper bound coming from the pulsar timing.

VI. THE QCD PHASE TRANSITION AND OUT-OF-EQUILIBRIUM SOUNDS

In this section, we discuss briefly the status of the debates on the order of the QCD phase transition. QCD with massless quarks has chiral symmetry, but in the real world finite quark masses make it only an approximate symmetry. Therefore, the transition to the broken phase does not need to be a real phase transition. We know from lattice gauge theory simulations that pure gauge SU(3) theory has the first order deconfinement transition. The other extreme – QCD with three massless quarks – also has the first order transition, now due to

the chiral symmetry restoration. However, for the real QCD, with physical values of u, d, s quark masses, the lattice results indicate, indeed, a smooth crossover-type transition (for current status of the problem see [5] and references therein).

However, the *deconfinement* is a more subtle story, with the conclusion much less obvious. Following the “dual superconductor” ideas of ’t Hooft and Mandelstam from 1980’s, the nature of confinement is the Bose-Einstein condensation of certain magnetically charged objects – color monopoles. Del Debbio *et al.* proposed an operator inserting a monopole into the vacuum. This operator has a nonzero vacuum expectation in the confined phase, as shown by the direct lattice simulation [22]. The behavior of the monopole Bose-clusters, which are interchange along the Matsubara circle – also indicate [23] that these objects undergo Bose-Einstein condensation at $T < T_c$. Thus, confinement indeed possesses certain observable “order parameters”. (Although in the usual “electric” formulation of the gauge theory those are non-local, they are local in models attempting its “magnetic” formulation.) Admittedly, two lattice works just mentioned are for pure gauge theories which do have phase transitions, not for QCD-like theories with quarks. The most accurate lattice simulations which focus on thermodynamical observables do show smoothening of the critical behavior by quark masses, and for physical QCD one finds so far is only a cross-over transition, without any visible singularity. (For a long time that was related to the fact that pure gauge theory are Z_N symmetric while theories with fundamental quarks are not: but discovery of confinement for gauge theories without center symmetry nullified this argument.)

So, there is no clear answer to the question of whether the deconfinement transition in physical QCD is a phase transition in the strict sense, only numerical limits. One possible resolution may be a “cryptic” transition, in which there is a singularity in the order parameter, which in thermodynamical observables is also present but too weak to be seen, with current numerical accuracy.

Another option for sound/GW generation is that while there is no first order transition in QCD, and therefore no mixed phase with macroscopically large bubbles, there may still exist some metastable objects in the near- T_c region with a lifetime large enough to cause out-of-equilibrium phenomena and sound generation. We recently studied dynamics of QCD strings and found [10] that certain nonperturbative objects, so-called “string balls”, can reach rather large mass in metastable states, which under a certain slow cooling can experience rapid collapse, similar to the gravitational collapse, due to the attractive self-interaction of QCD strings. Such collapse can also generate inhomogeneous energy distribution, “overcooling” and subsequent sound generation.

The freezeout in the Little Bang is happening very close to the QCD phase transition region. Studies of rapidity correlation among secondaries reveal existence of clustering of secondaries, perhaps local remnants of QGP

phase. Study of this process leads to suggestion [21] – not yet observed – that such QGP clusters should implode at $T < T_c$, in what was called “mini-bangs”. Such process may be a very effective mechanism of transferring energy into sounds. Note, however, that since the speeds of sounds passing through the medium in the Little and Big Bangs cases are vastly different, the numbers involved and perhaps even the qualitative dynamics may be quite different.

VII. SUMMARY AND DISCUSSION

In this paper we discussed cosmological production of gravity waves from the sound waves, originating in the Big Bang phase transitions. While most of studies focus on the electroweak transition, we instead emphasized the QCD one. The main reasons for that are our background and the expected progress in pulsar timing and correlation technique, which may make a detection of cosmological GW possible in the near future.

One our conclusion is that, as a function of momentum scale k , there should be three distinct stages: (i) initial generation of the sound spectrum at the “UV root” scale $k \sim T$, (ii) weak acoustic turbulence, with two distinct scenarios – with and without sound decays – followed by (iii) conversion of sounds into GW. While (i) stage is highly nontrivial and requires further studies, we argue that the intermediate regime (ii) is reasonably well understood theoretically.

We also find that the process of GW generation itself can be calculated using the one-loop sound diagram for the stress tensor correlator and standard rules of its calculation. Furthermore, the loop diagram can be cut by unitarity, putting the sound waves on-shell. The only needed additional ingredient remains the occupancy factors: the GW yield is proportional to its square at the appropriate momenta.

We argue that the weak acoustic inverse cascade can drastically amplify the sounds, as one decreases k , due to the large value of the index. Therefore, the requirements on the UV sources of the sound can be greatly reduced.

However, a certain mechanism producing sounds is still needed. Out-of-equilibrium dynamics of QCD and EW phase transition remains far from being understood. We argued above that certain order parameter do jump at T_c , small-latent-heat deconfinement transition of the first order is still perhaps possible: if so, there would be mixed phase and bubbles, alight with relatively small contrast in the energy density between the phases. It was so far assumed in literature that bubble walls must collide to produce the sounds. However, there is another potential mechanism, well known in hydrodynamical literature, namely the Rayleigh-type collapse of the QGP clusters at $T < T_c$ [21]. One more possibility we mention is a crossover transition, with only microscopic metastable objects – e.g. the string balls [10] – producing the out-of-equilibrium sounds.

Acknowledgements. This work was supported in part by the U.S. Department of Energy under Contract

No. DE-FG-88ER40388.

-
- [1] M. Hindmarsh, S. J. Huber, K. Rummukainen and D. J. Weir, Phys. Rev. Lett. **112**, 041301 (2014) [arXiv:1304.2433 [hep-ph]].
- [2] E. Witten, Phys. Rev. D **30**, 272 (1984).
- [3] C. J. Hogan, Mon. Not. Roy. Astron. Soc. **218**, 629 (1986).
- [4] M. Lublinsky and E. Shuryak, Phys. Rev. D **80**, 065026 (2009) [arXiv:0905.4069 [hep-ph]].
- [5] T. Bhattacharya, M. I. Buchoff, N. H. Christ, H.-T. Ding, R. Gupta, C. Jung, F. Karsch and Z. Lin *et al.*, Phys. Rev. Lett. **113**, 082001 (2014) [arXiv:1402.5175 [hep-lat]].
- [6] P. Staig and E. Shuryak, Phys. Rev. C **84**, 044912 (2011) [arXiv:1105.0676 [nucl-th]].
- [7] C. Gale, S. Jeon and B. Schenke, Int. J. Mod. Phys. A **28**, 1340011 (2013) [arXiv:1301.5893 [nucl-th]].
- [8] P. Romatschke, Prog. Theor. Phys. Suppl. **174** (2008) 137 [arXiv:0710.0016 [nucl-th]].
- [9] Musielak, Z. E., Rosner, R., Stein, R. F., & Ulmschneider, P. 1994, Astrophys. J. , 423, 474
- [10] T. Kalaydzhyan and E. Shuryak, Phys. Rev. D **90**, 025031 (2014) [arXiv:1402.7363 [hep-ph]].
- [11] J. Liao and E. Shuryak, Phys. Rev. C **75**, 054907 (2007) [hep-ph/0611131].
- [12] M. N. Chernodub and V. I. Zakharov, Phys. Rev. Lett. **98**, 082002 (2007) [hep-ph/0611228].
- [13] G. Basar, D. E. Kharzeev and E. V. Shuryak, Phys. Rev. C **90**, 014905 (2014) [arXiv:1402.2286 [hep-ph]].
- [14] P. Kovtun, G. D. Moore and P. Romatschke, Phys. Rev. D **84**, 025006 (2011) [arXiv:1104.1586 [hep-ph]].
- [15] P. Kovtun, J. Phys. A **45**, 473001 (2012) [arXiv:1205.5040 [hep-th]].
- [16] R. M. Shannon, V. Ravi, W. A. Coles, G. Hobbs, M. J. Keith, R. N. Manchester, J. S. B. Wyithe and M. Bailes *et al.*, Science **342** (2013) 6156, 334 [arXiv:1310.4569 [astro-ph.CO]].
- [17] E. V. Shuryak, Phys. Lett. B **78**, 150 (1978) [Sov. J. Nucl. Phys. **28**, 408 (1978)] [Yad. Fiz. **28**, 796 (1978)].
- [18] V.E. Zakharov, V.S. Lvov, G. Falkovich, “Kolmogorov spectra of turbulence I. Wave turbulence.”, Springer Verlag. ISBN 3-540-54533-6.
- [19] R. Micha and I. I. Tkachev, Phys. Rev. D **70**, 043538 (2004) [hep-ph/0403101].
- [20] J. Berges, K. Boguslavski, S. Schlichting and R. Venugopalan, Phys. Rev. D **89**, 074011 (2014) [arXiv:1303.5650 [hep-ph]].
- [21] E. Shuryak and P. Staig, Phys. Rev. C **88**, no. 6, 064905 (2013) [arXiv:1306.2938 [nucl-th]].
- [22] L. Del Debbio, A. Di Giacomo, G. Paffuti and P. Pieri, Phys. Lett. B **355**, 255 (1995) [hep-lat/9505014].
- [23] A. D’Alessandro, M. D’Elia and E. V. Shuryak, Phys. Rev. D **81**, 094501 (2010) [arXiv:1002.4161 [hep-lat]].
- [24] Note that we use not gravitational but particle physics units, in which $c=1$ but the Newton constant $G_N = 1/M_p^2$.